

Split of the pseudo-critical temperatures of chiral and confine/deconfine transitions by temperature gradient

Ji-Chong Yang,^{*} Wen-Wen Li,[†] and Chong-Xing Yue[‡]

Department of Physics, Liaoning Normal University, Dalian 116029, China and

Center for Theoretical and Experimental High Energy Physics,

Liaoning Normal University, Dalian 116029, China

(Dated: January 9, 2024)

arXiv:2401.03826v1 [hep-lat] 8 Jan 2024

Abstract

Searching of the critical endpoint of the phase transition of Quantum Chromodynamics (QCD) matter in experiments is of great interest. The temperature in the fireball of a collider is location dependent, however, most theoretical studies address the scenario of uniform temperature. In this work, the effect of temperature gradients is investigated using lattice QCD approach. We find that the temperature gradient catalyzes chiral symmetry breaking, meanwhile the temperature gradient increases the Polyakov loop in the confined phase but suppresses the Polyakov loop in the deconfined phase. Furthermore, the temperature gradient decreases the pseudo-critical temperature of chiral transition but increases the pseudo-critical temperature of the confine/deconfine transition.

I. INTRODUCTION

The study of the phase diagram of Quantum Chromodynamics (QCD) is motivated by the desire to understand the fundamental properties of strongly interacting matter under extreme conditions. QCD is the theory that describes the strong interaction and the behavior of quarks and gluons, which are the building blocks of protons, neutrons, and other hadrons. By exploring the phase diagram, which represents the different phases of matter as a function of temperature and baryon chemical potential, one can gain insights into the behavior of matter at high temperatures and densities [1], such as those present in the early universe [2], neutron stars [3], and heavy-ion collisions [4, 5]. Not only that, the study of QCD phase transitions is one of the important ways to explore the color confinement.

The precise determination of phase transition temperatures and the location of the critical point in QCD remains challenging. Experimental observations, provide indirect information about the QCD phase diagram through the analysis of particle spectra, yields, and correlations. These experimental observables can be used to infer the properties of the system, however, a direct mapping between experimental observables and theoretical phase transition temperatures is not straightforward and requires careful analysis and comparison. There are other obstacles in the middle of theory and experiment, for example, phase transition theory studies are mainly focused on equilibrium states while there is non-equilibrium effect

* yangjichong@lnnu.edu.cn

† lww1514148@163.com

‡ cxyue@lnnu.edu.cn; Corresponding author

in experiments, and also the fact that the experimental situation is much more complicated, with issues such as finite volumes, position-dependent temperatures and baryon number densities [5, 6].

Typically, in a heavy ion collider, the quark-gluon-plasma (QGP) and the hadronic phase are separated by a dynamical phase transition surface in a fireball, which is located in a region of nonuniform temperature. It has been studied using Ising-like effective potential that the temperature gradient will lift the critical temperature [6]. Ref. [6] studies the situation of a brick cell of the fireball, in which there is a difference in the spatial distribution of temperature, and the stationary phase transition surface in a steady temperature-nonuniform system is studied. In this work, a similar situation is considered using lattice QCD approach with $N_f = 2$ (two degenerate flavors) dynamic staggered fermions. The nonuniform temperature is introduced with the help of nonuniform lattice spacings.

In hot QCD, there are two types of phase transitions in the $T - \mu$ plane where T is temperature and μ denotes the chemical potential. In the case of chiral fermion, there is the chiral symmetry phase transition, and the corresponding order parameter is the chiral condensation. In the case where dynamic fermions are absent, there is the confine/deconfine phase transition, the corresponding order parameter is the Polyakov loop. For finite fermion mass, both transitions are crossovers. For a long time, these two transitions were considered to occur simultaneously, except for the case of quarkyonic phase in the high baryon density region [7]. The pseudo-critical temperatures of the two transitions are close to each other in the lattice studies [8], and the discrepancy between the two has been attributed to the nature of crossovers. Studies have been devoted to investigate the interplay of the two in order to understand the nature of the phase transition of hot QCD matter [9]. In this work, the chiral condensation, Polyakov loop as well as the pseudo-critical temperature are studied with the focus on the shift of the pseudo-critical temperature. However, we find that, in the case of zero baryon density, the temperature gradient causes the pseudo-critical temperatures of the two transitions to move away from each other, which is a phenomenon worth noting.

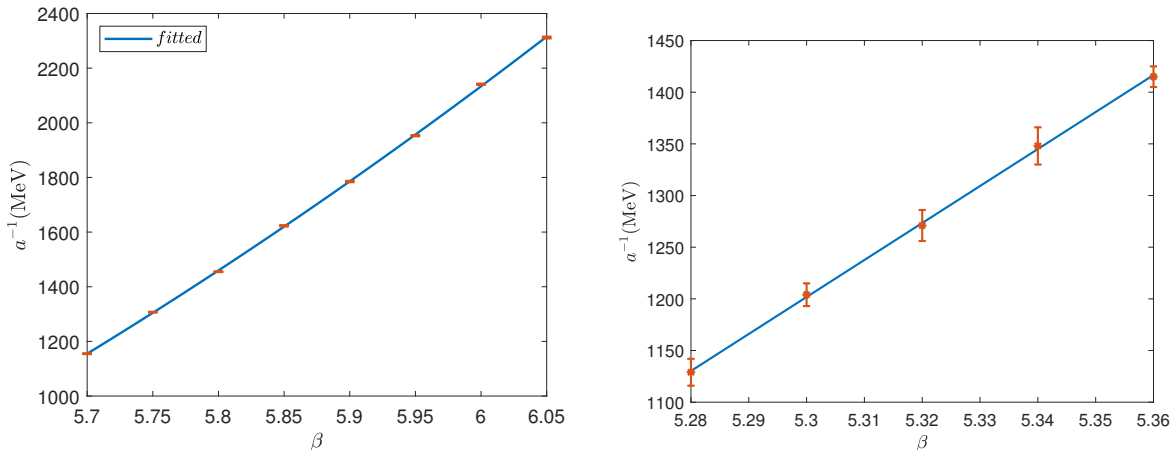


FIG. 1. The lattice spacing as a function of β , and the fitted results. The left panel is for the quenched approximation, the right panel is for the case when dynamic fermions are turned on.

II. LATTICE SETUP AND PARAMETERS

In this work, both the case of quenched approximation and the case of $N_f = 2$ dynamic fermions are studied. When the dynamic fermions are turned on, the Kogut-Susskind staggered fermions [10] are used, the action is $S = S_G + S_q$, and,

$$\begin{aligned}
 S_G &= \frac{\beta(n_z)}{N_c} \sum_n \sum_{\mu > \nu} \text{Re tr} [1 - \bar{U}_{\mu\nu}(n)], \\
 S_q &= \sum_n \left(\sum_{\mu} \sum_{\delta = \pm\mu} \bar{\chi}(n) U_{\delta}(n) \eta_{\delta}(n) \chi(n + \delta) \right. \\
 &\quad \left. + 2am \bar{\chi} \chi \right),
 \end{aligned} \tag{1}$$

where a is the lattice spacing, m is the fermion mass with $am = 0.1$ which is heavier than the physical mass, but lighter as a computational resource needed for exploratory research, $U_{\mu} = e^{iaA_{\mu}}$, $\eta_{\mu}(n) = (-1)^{\sum_{\nu < \mu} n_{\nu}}$, $U_{-\mu}(n) = U_{\mu}^{\dagger}(n - \mu)$, $\eta_{-\mu} = -\eta_{\mu}(n - \mu)$, and $\bar{U}_{\mu\nu}(n) = (U_{\mu,\nu}(n) + U_{\mu,-\nu}(n) + U_{-\mu,\nu}(n) + U_{-\mu,-\nu}(n)) / 4$ where $U_{\mu,\nu}(n) = U_{\mu}(n) U_{\nu}(n + \mu) U_{-\mu}(n + \nu) U_{-\nu}(n)$. The rational hybrid Monte Carlo [11] is used to implement the ‘forth root trick’.

Note that, β is introduced as a function of n_z , so that the lattice spacing is a function of n_z . The effect of simulating temperature gradient along the z -axis is achieved by assigning different lattice spacings for different z -slices along the z -axis, i.e., the whole volume is a

number of z -slices with different temperatures stacked together. It is worth noting that in this way, for different z -slices, the lattice spacings, the extents in $x - y$ directions, and quark masses are also different. In this work, we ignore these differences mentioned above, and assume that the main factor of the variation due to different lattice spacing is from the difference in temperature.

To find out the temperatures corresponding to different values of β , matching is carried out using a $L_x \times L_y \times L_z \times L_\tau = 12^3 \times 48$ lattice, where $L_{x,y,z,\tau}$ are extents at different directions. When dynamic fermions are turned on, $am = 0.1$ is used. For quenched approximation, $(200 + 9800)$ molecular dynamics time units (TUs) are simulated for each β with $\beta = 5.7 + 0.05k$, where $0 \leq k \leq 7$ are integers, 200 trajectories of the 10000 configurations are used for thermalization and 9800 trajectories are measured. When dynamic fermions are turned on, $(200 + 1000)$ configurations are generated for each β with $\beta = 5.28, 5.3, 5.32, 5.34$ and 5.36 , where 200 trajectories are used for thermalization and 1000 trajectories are measured. The lattice spacing a is determined by measuring the static quark potential $V(r)$ [12] and then matching the ‘Sommer scale’ r_0 to 0.5 fm [13].

In order to cover the values of β where no matching was performed, and also to compute the derivative of the temperature w.r.t. n_z , the dependence of a^{-1} on β was fitted to a function, under the assumption that the range of β is small enough and that the first few orders of the Taylor expansion are sufficient to characterize this relationship. In the case of quenched approximation, a bilinear function is sufficient. When dynamic fermions are turned on, the range of β is small enough that it is sufficient to consider only the linear order of the Taylor expansion. The results of the fittings are shown in Fig. 1, and can be written as,

$$\begin{aligned} \left. \frac{a^{-1}}{\text{MeV}} \right|_{\text{Quench}} &= 19451.4 - 9357.7\beta + 1078.6\beta^2, \\ \left. \frac{a^{-1}}{\text{MeV}} \right|_{N_f=2} &= -17772.2 + 3580.0\beta. \end{aligned} \tag{2}$$

We focus on the Polyakov loop and chiral condensation and their susceptibilities. The

quantities are defined as [14],

$$\begin{aligned}
P &= \frac{1}{N_c L_x L_y L_z} \sum_{\vec{n}} \prod_{n_\tau} U_\tau(\vec{n}), \\
\chi_P &= a^3 L_x L_y L_z (\langle P^2 \rangle - \langle P \rangle^2), \\
c &= -\frac{1}{a^3 L_x L_y L_z L_\tau} \text{tr}[D^{-1}], \\
\chi_{disc} &= \frac{1}{a^2 L_x L_y L_z L_\tau} \left(\langle \text{tr}[D^{-1}]^2 \rangle - \langle \text{tr}[D^{-1}] \rangle^2 \right),
\end{aligned} \tag{3}$$

where P is the bare Polyakov loop, c is the bare chiral condensation, χ_P is the susceptibility of P , and χ_{disc} is the disconnected susceptibility of the bare chiral condensation. In the case of quenched approximation, we use $\chi_{|P|} = a^3 L_x L_y L_z (\langle |P|^2 \rangle - \langle |P| \rangle^2)$. When there is a temperature gradient, we focus on simulations on a lattice with $L_x L_y L_z L_\tau = 12^3 \times 6$. In the uniform temperature case, $2000 + (100 + 49900) \times 8$ TUs are simulated, where 50000 TUs are simulated for each value of β sequentially with β growing, except for the first value of β that 52000 TUs are simulated. The last 49900 configurations for each value of β are measured. In the quenched approximation, $\beta = 5.7 + 0.05k$, in the $N_f = 2$ case, $\beta = 5.29 + 0.01 \times k$, both with $0 \leq k \leq 7$. At the above parameters, the susceptibilities χ_P and χ_{disc} are shown in Fig. 2. The (pseudo-)critical temperatures of the transitions can be obtained using the peaks of the susceptibilities.

Through out this paper, we use $\sigma = \sqrt{2\tau_{\text{int}}}\sigma_{\text{jk}}$ as statistical error [15], where τ_{int} is the separation of TUs such that the two configurations can be regarded as independent, and σ_{jk} is statistical error calculated using ‘jackknife’ method. τ_{int} is calculated by using ‘autocorrelation’ with $S = 1.5$ [16] on the bare Polyakov loop or the bare chiral condensation depending on whether we are measuring quantities w.r.t. Polyakov loop or chiral condensation. The one exception is the lattice spacing, where the statistical error is calculated using τ_{int} estimated from the bare Polyakov loop.

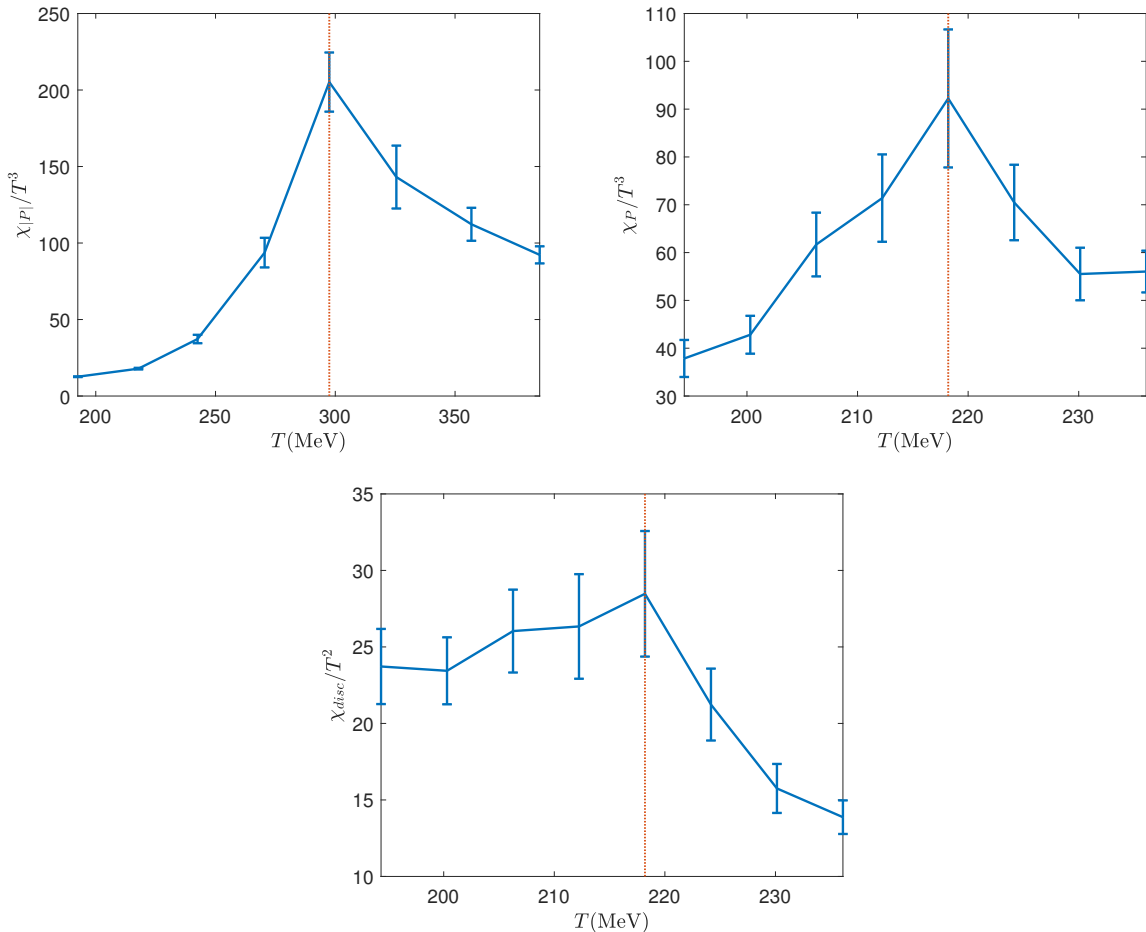


FIG. 2. The susceptibilities as functions of temperature. The top left panel is $\chi_{|P|}$ in quenched approximation. The top right panel is χ_P and the bottom panel is χ_{disc} when dynamic fermions are turned on. The dotted line in the top left panel shows the critical temperature of the confined/deconfine phase transition, and in the other two panels show the pseudo-critical temperatures of the transitions.

III. NUMERICAL RESULTS FOR THE CASE OF TEMPERATURE GRADIENT

Since in our simulation, β is a function of z , the quantities in a z -slice are also interested. They are defined as,

$$\begin{aligned}
 P_z(n_z) &= \frac{1}{N_c L_x L_y} \sum_{n_{x,y}} \prod_{n_\tau} U_\tau(\vec{n}), \\
 c_z(n_z) &= -\frac{1}{a^3 L_x L_y L_\tau} \sum_{n_{x,y,\tau}} D^{-1}(n|n).
 \end{aligned}
 \tag{4}$$

The origin of the coordinate is chosen such that $0 \leq n_z \leq 11$, and,

$$\beta(n_z) = \beta_0 + \Delta\beta \sin\left(\frac{2n_z\pi}{L_z}\right), \quad (5)$$

where $L_z = 12$ is the extent on the z direction. The reason we use a periodic function for $\beta(n_z)$ is to avoid the analysis of possible effects from the boundary. In the case of quenched approximation, the fermion mass is infinite, and thus receives no effect from the change of lattice spacing. As a way to explore the effect of the temperature gradient, we intentionally choose a large temperature gradient, only $\Delta\beta = 0.5$ is studied. In the case of $N_f = 2$ dynamic fermions, to study the shift of the pseudo-critical temperature, four cases are considered such that $\Delta\beta = 0.05, 0.1, 0.15$ and 0.2 . The β_0 are as same as β used in previous section, and the number of configurations for each $\Delta\beta$ are also as same as those in the previous section, therefore the results of the previous section consist as the case of $\Delta\beta = 0$. The temperature gradient can be calculated as,

$$\frac{\partial T}{\partial z} = \frac{2\Delta\beta\pi}{aL_\tau L_z} \cos\left(\frac{2n_z\pi}{L_z}\right) \frac{\partial a^{-1}}{\partial \beta}. \quad (6)$$

A. Effect of temperature gradient on Polyakov loop and chiral condensation

A naive conjecture is that neither the chiral condensation nor the Polyakov loop should depend on the direction of the temperature gradient. This can be verified by comparing the chiral condensation and Polyakov loop at $n_z = 0$ and $n_z = 6$. For quenched approximation, and for N_f with $\Delta\beta = 0.2$, the chiral condensation and Polyakov loop are shown in Fig. 3. In quenched approximation, chiral condensation is not order parameter, but the result is still shown. It can be seen that the difference between $n_z = 0$ and $n_z = 6$ is negligible even when the temperature gradient is very large. Therefore, in the following, $n_z = 0$ and $n_z = 6$ are combined together, i.e., we use $P^{(\Delta\beta)} = (P_z(0) + P_z(6))/2$, and $c^{(\Delta\beta)} = (c_z(0) + c_z(6))/2$, in the case of quenched approximation, we also considered $\tilde{P}^{(\Delta\beta)} = (|P_z(0)| + |P_z(6)|)/2$.

Note that, at $n_z = 0, 6$, $\beta(n_z) = \beta_0$, so $P^{(\Delta\beta)}$ and $c^{(\Delta\beta)}$ are Polyakov loops and chiral condensations at β_0 with different temperature gradients. At $n_z = 0, 6$, $|\partial T/\partial z| = (\Delta\beta\pi a^{-1} |\partial a^{-1}/\partial \beta|)/36$. In quenched approximation, $\Delta\beta = 0.5$ corresponds to the range of temperature gradient from $|\partial T/\partial z| = (385 \text{ MeV})^2$ ($\beta = 5.7$) to $|\partial T/\partial z| = (611 \text{ MeV})^2$ ($\beta = 6.05$). In the case of $N_f = 2$ and $\Delta\beta = 0.05$, the range of temperature gradient is from

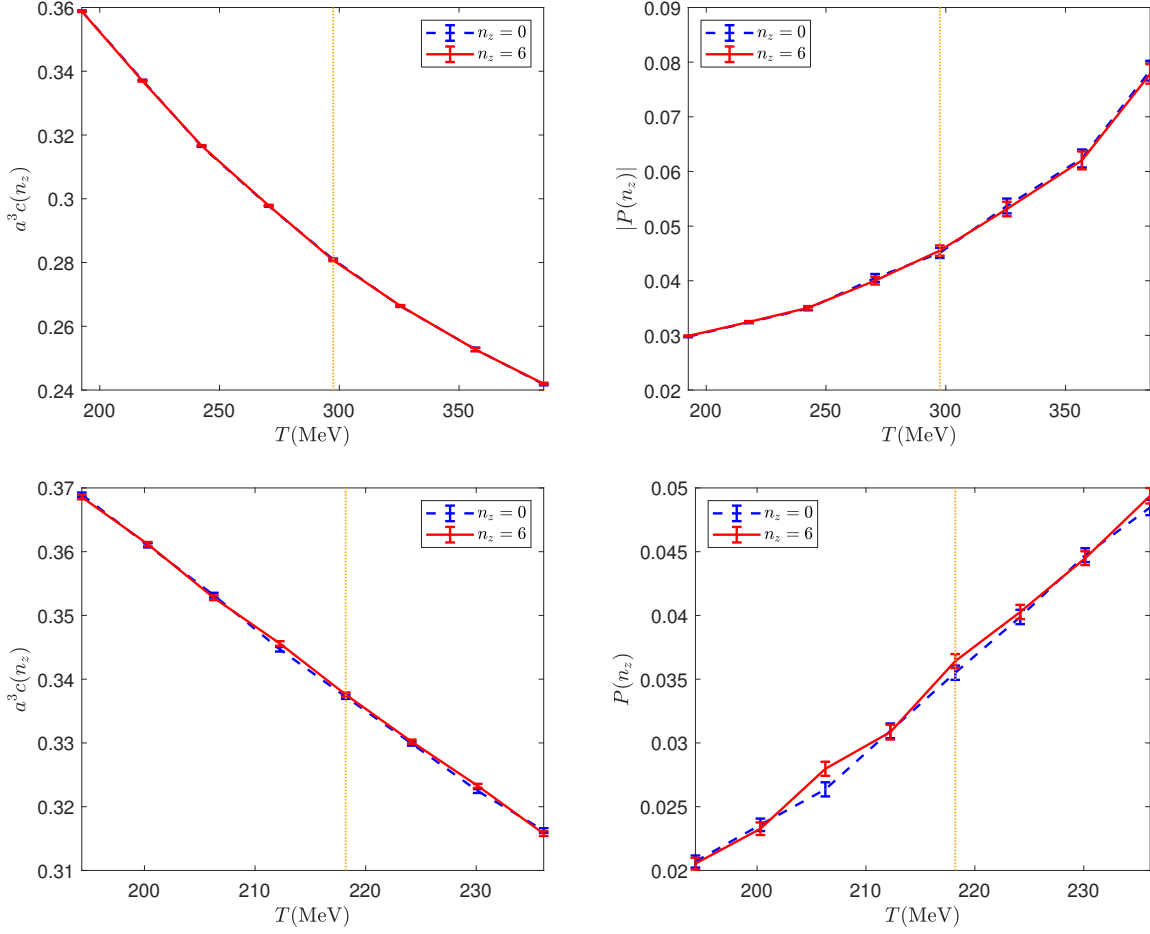


FIG. 3. $\langle c(n_z) \rangle$, $\langle |P(n_z)| \rangle$ and $\langle P(n_z) \rangle$ at $n_z = 0$ and 6. The first row is for quenched approximation, where the left panel is $\langle c(n_z) \rangle$, the right panel is $\langle |P(n_z)| \rangle$. The second row is for the case when dynamic fermions are turned on, where the left panel is $\langle c(n_z) \rangle$, the right panel is $\langle P(n_z) \rangle$. The dotted lines show the (pseudo)-critical temperatures of the transitions for the case of uniform temperature.

$|\partial T / \partial z| = (135 \text{ MeV})^2$ ($\beta = 5.29$) to $|\partial T / \partial z| = (149 \text{ MeV})^2$ ($\beta = 5.36$). The ranges of temperature gradient for the cases of $\Delta\beta = 0.1, 0.15$, and 0.2 are two, three and four times of the case for $\Delta\beta = 0.05$, respectively.

$\langle c^{(\Delta\beta)} \rangle$, $\langle |P^{(\Delta\beta)}| \rangle$ and $\langle \tilde{P}^{(\Delta\beta)} \rangle$ in quenched approximation are shown in Fig. 4. It can be shown that, the temperature gradient always increase the chiral condensation, while only suppress the Polyakov loop in the deconfined phase. Note that, in the quenched approximation, the temperature gradient is set to be large. A noteworthy phenomenon is that,

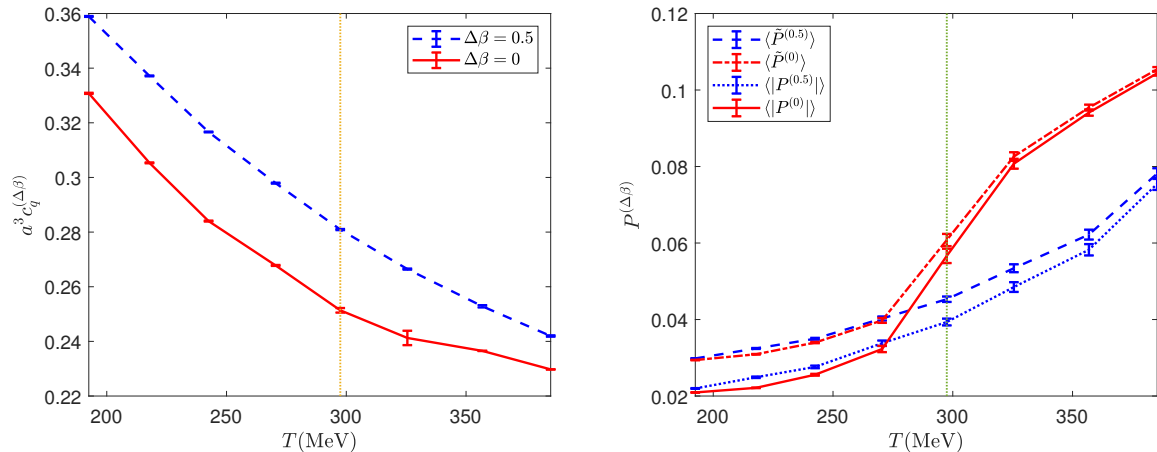


FIG. 4. $\langle c^{(\Delta\beta)} \rangle$ (left panel), $\langle |P^{(\Delta\beta)}| \rangle$ and $\langle \tilde{P}^{(\Delta\beta)} \rangle$ (right panel) as functions of T in quenched approximation. The dotted lines show the critical temperature of the confine/deconfine phase transition for the case of uniform temperature.

in the confined phase, a large temperature gradient barely affects the Polyakov loop. Assuming that the distribution of temperature is continuous, the derivatives (at every order) of temperature at a given location taken together essentially respond to the distribution of temperature in the region around that location. Therefore, the effect of the temperature gradient actually reflects the effect of temperature distribution at subleading order. When viewed as a whole, the phenomenon essentially comes from the distribution of temperature. Thus, it can be speculated that in the confined phase and without dynamic fermions, the gluon field is hardly affected by the distant gluon field, while it is not true in the deconfined phase.

When dynamic fermions are turned on, the results are shown in Fig. 5. It can be seen from the results that for chiral condensation, temperature gradient always leads to chiral symmetry breaking, and larger temperature gradient leads to larger chiral symmetry breaking. Meanwhile, the temperature gradient can increase Polyakov loop at low temperatures and decrease Polyakov loop at high temperatures. Moreover, the curves of Polyakov loop versus temperature for different temperature gradients intersect with the curve in the uniform temperature case approximately near the pseudo-critical temperature of the confine/deconfine transition for the uniform temperature case. Thus it can be concluded that the temperature gradient contributes to the deconfinement in the confined phase, and the opposite is true in

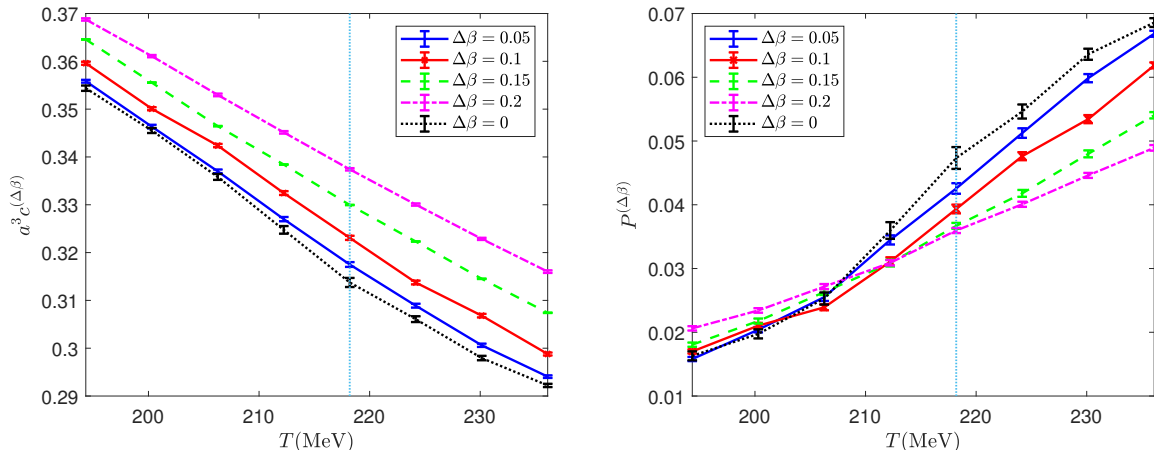


FIG. 5. $\langle c^{(\Delta\beta)} \rangle$ (left panel) and $\langle P^{(\Delta\beta)} \rangle$ (right panel) at different temperatures and different temperature gradients. The dotted lines show the pseudo-critical temperature of the transitions for the case of uniform temperature.

the deconfined phase. A noteworthy phenomenon is that in the confined phase, temperature gradient can increase both chiral condensation and Polyakov loop.

B. Shift of phase transition with $N_f = 2$ staggered fermions

To investigate the phase transition, the susceptibilities with the temperature gradient is defined as,

$$\begin{aligned}\chi_P^{(\Delta\beta)} &= 2a^3 L_x^2 \left(\langle (P^{(\Delta\beta)})^2 \rangle - \langle P^{(\Delta\beta)} \rangle^2 \right), \\ \chi_{disc}^{(\Delta\beta)} &= 2a^4 L_x^2 L_\tau \left(\langle (c^{(\Delta\beta)})^2 \rangle - \langle c^{(\Delta\beta)} \rangle^2 \right).\end{aligned}\tag{7}$$

In Eq. (7), the $n_z = 0$ and $n_z = 6$ z -slices are combined as a $12^2 \times 2 \times 6$ lattice. For quenched approximation, $\chi_{|P|}^{(\Delta\beta)}$ and $\chi_{\tilde{P}}^{(\Delta\beta)}$ are defined as same as Eq. (7) except that $P^{(\Delta\beta)}$ is substituted by $|P^{(\Delta\beta)}|$ and $\tilde{P}^{(\Delta\beta)}$.

For quenched approximation, the peaks of $\chi_{|P|}^{(\Delta\beta)}$ and $\chi_{\tilde{P}}^{(\Delta\beta)}$ are shown in Fig. 6. When dynamic fermions are turned on, the susceptibilities of the chiral condensation ($\chi_P^{(\Delta\beta)}$) and Polyakov loop ($\chi_{disc}^{(\Delta\beta)}$) as functions of temperature at different temperature gradients are shown in Fig. 7. It can be shown that, for $\Delta\beta = 0$, the positions of the peaks of susceptibilities defined using $n_z = 0, 6$ are consistent with the susceptibilities of the whole lattice.

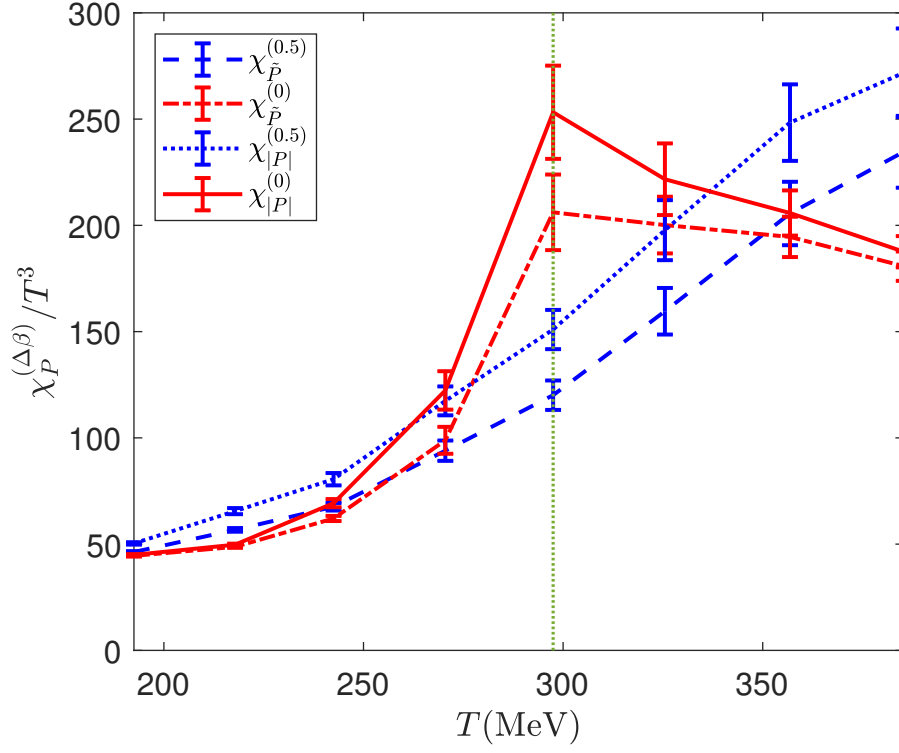


FIG. 6. $\chi_{|P|}^{(\Delta\beta)}$ and $\chi_{\bar{P}}^{(\Delta\beta)}$ as functions of T in quenched approximation. The dotted lines show the critical temperature for the case of uniform temperature.

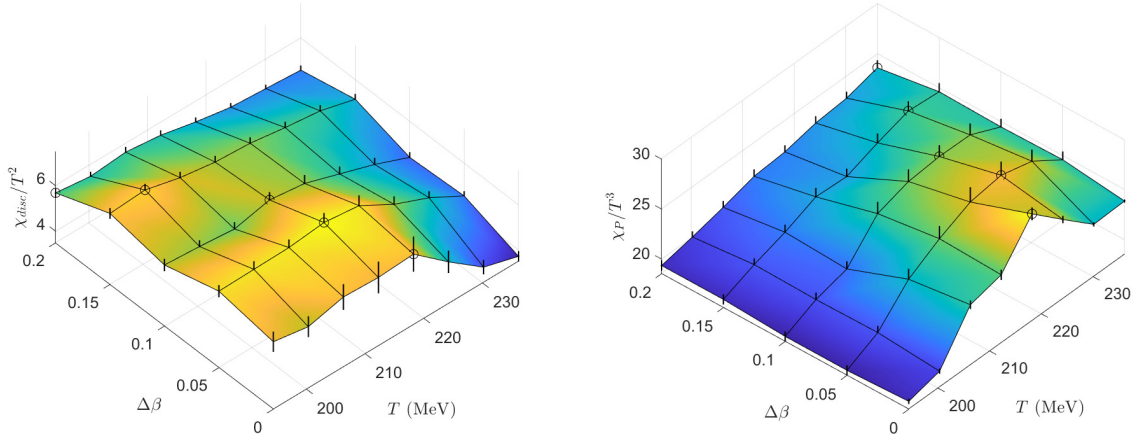


FIG. 7. $\chi_{disc}^{(\Delta\beta)}$ (left panel) and $\chi_P^{(\Delta\beta)}$ (right panel) as functions of temperature at different temperature gradients. For each fixed $\Delta\beta$, the highest peaks of susceptibilities are marked with small circles.

For quenched approximation, when $\Delta\beta = 0.5$ the peak is pushed towards a higher temperature, which is consistent with the behavior that the temperature gradient will suppress the Polyakov loop in the deconfined phase, and is consistent with the model prediction [6].

In Fig. 7, for each fixed $\Delta\beta$, the highest peaks of susceptibilities are marked with small circles. It can be seen that for the chiral condensation, the peak of the susceptibility moves to a lower temperature with the increase of the temperature gradient, meanwhile, for the Polyakov loop, the peak of the susceptibility moves to a higher temperature. In other words, the temperature gradient causes the pseudo-critical temperatures of the confine/deconfine transition and the chiral symmetry breaking transition to move away from each other.

As can be seen from the susceptibility of the Polyakov loop, the temperature gradient broadens and softens the peak of the susceptibility. Notice that for the $\Delta\beta = 0$ case, Fig. 7 shows the susceptibility also defined with $n_z = 0, 6$, so this broadening is not due to the smaller volume. Similar to finite volume, a temperature gradient also pulls the system away from the singularity, which, together with the system's cross-over feature, makes the order parameter more ill-defined. This may explain the fact that the shift of peaks of susceptibilities for chiral condensation are inconsistent with the change of chiral condensation. This phenomenon reflects the fact that the chiral condensation is no longer a suitable order parameter when a temperature gradient presents.

IV. SUMMARY

In colliders, the fireball is at a location dependent temperature distribution instead of a uniform temperature. In this work, the presence of temperature gradient is studied using lattice QCD approach with location dependent β .

In quenched approximation, the temperature gradient always catalyzes the chiral symmetry breaking. Meanwhile, the Polyakov loop is suppressed by the temperature gradient, but this only happens in the deconfined phase, in the confined phase, the Polyakov loop is barely affected by the temperature gradient. The temperature gradient will increase the critical temperature of confine/deconfine phase transition, which is consistent with the model prediction.

When dynamic fermions are turned on, the temperature gradient still catalyzes the chiral symmetry breaking. However, the Polyakov loop is increased in the deconfined phase, while

decreased in the confined phase, i.e., in the confined phase, the chiral condensation and the Polyakov loop are increased at the same time. Not only that, but the pseudo-critical temperatures of the chiral symmetry breaking transition and the confine/deconfine transition move in the opposite direction. Although the chiral symmetry breaking is catalyzed, the pseudo-critical temperature is lowered down. Since temperature gradient broadens and softens the peaks of susceptibilities, it is suggested that the order parameter may be questioned, however, a fully understanding of these phenomena will require future theoretical studies.

ACKNOWLEDGMENTS

This work was supported in part by the National Natural Science Foundation of China under Grants Nos. 11875157 and 12147214, and the Natural Science Foundation of the Liaoning Scientific Committee No. LJKZ0978.

-
- [1] K. Fukushima and C. Sasaki, The phase diagram of nuclear and quark matter at high baryon density, *Prog. Part. Nucl. Phys.* **72**, 99 (2013), [arXiv:1301.6377 \[hep-ph\]](#); W. Busza, K. Rajagopal, and W. van der Schee, Heavy Ion Collisions: The Big Picture, and the Big Questions, *Ann. Rev. Nucl. Part. Sci.* **68**, 339 (2018), [arXiv:1802.04801 \[hep-ph\]](#); A. Bzdak, S. Esumi, V. Koch, J. Liao, M. Stephanov, and N. Xu, Mapping the Phases of Quantum Chromodynamics with Beam Energy Scan, *Phys. Rept.* **853**, 1 (2020), [arXiv:1906.00936 \[nucl-th\]](#).
 - [2] P. Braun-Munzinger and J. Wambach, The Phase Diagram of Strongly-Interacting Matter, *Rev. Mod. Phys.* **81**, 1031 (2009), [arXiv:0801.4256 \[hep-ph\]](#); P. Braun-Munzinger, V. Koch, T. Schäfer, and J. Stachel, Properties of hot and dense matter from relativistic heavy ion collisions, *Phys. Rept.* **621**, 76 (2016), [arXiv:1510.00442 \[nucl-th\]](#).
 - [3] D. Page and S. Reddy, Dense Matter in Compact Stars: Theoretical Developments and Observational Constraints, *Ann. Rev. Nucl. Part. Sci.* **56**, 327 (2006), [arXiv:astro-ph/0608360](#); J. M. Lattimer and M. Prakash, The Equation of State of Hot, Dense Matter and Neutron Stars, *Phys. Rept.* **621**, 127 (2016), [arXiv:1512.07820 \[astro-ph.SR\]](#).
 - [4] M. M. Aggarwal *et al.* (STAR), An Experimental Exploration of the QCD Phase Diagram: The Search for the Critical Point and the Onset of De-confinement (2010) [arXiv:1007.2613 \[nucl-ex\]](#);

- A. Andronic, P. Braun-Munzinger, K. Redlich, and J. Stachel, Decoding the phase structure of QCD via particle production at high energy, *Nature* **561**, 321 (2018), [arXiv:1710.09425 \[nucl-th\]](#); X. Luo, S. Shi, N. Xu, and Y. Zhang, A Study of the Properties of the QCD Phase Diagram in High-Energy Nuclear Collisions, *Particles* **3**, 278 (2020), [arXiv:2004.00789 \[nucl-ex\]](#).
- [5] M. Abdallah *et al.* (STAR), Cumulants and correlation functions of net-proton, proton, and antiproton multiplicity distributions in Au+Au collisions at energies available at the BNL Relativistic Heavy Ion Collider, *Phys. Rev. C* **104**, 024902 (2021), [arXiv:2101.12413 \[nucl-ex\]](#).
- [6] J.-H. Zheng and L. Jiang, Nonuniform-temperature effects on the phase transition in an Ising-like model, *Phys. Rev. D* **104**, 016031 (2021), [arXiv:2102.11154 \[nucl-th\]](#).
- [7] L. McLerran and R. D. Pisarski, Phases of cold, dense quarks at large $N(c)$, *Nucl. Phys. A* **796**, 83 (2007), [arXiv:0706.2191 \[hep-ph\]](#).
- [8] J. B. Kogut, M. Stone, H. W. Wyld, W. R. Gibbs, J. Shigemitsu, S. H. Shenker, and D. K. Sinclair, Deconfinement and Chiral Symmetry Restoration at Finite Temperatures in SU(2) and SU(3) Gauge Theories, *Phys. Rev. Lett.* **50**, 393 (1983); M. Fukugita and A. Ukawa, Deconfining and Chiral Transitions of Finite Temperature Quantum Chromodynamics in the Presence of Dynamical Quark Loops, *Phys. Rev. Lett.* **57**, 503 (1986); F. Karsch and E. Laermann, Susceptibilities, the specific heat and a cumulant in two flavor QCD, *Phys. Rev. D* **50**, 6954 (1994), [arXiv:hep-lat/9406008](#); S. Dital, E. Laermann, and H. Satz, Deconfinement through chiral symmetry restoration in two flavor QCD, *Eur. Phys. J. C* **18**, 583 (2001), [arXiv:hep-ph/0007175](#); Interplay between chiral transition and deconfinement, *Nucl. Phys. A* **702**, 159 (2002); C. Bernard, T. Burch, E. B. Gregory, D. Toussaint, C. E. DeTar, J. Osborn, S. Gottlieb, U. M. Heller, and R. Sugar (MILC), QCD thermodynamics with three flavors of improved staggered quarks, *Phys. Rev. D* **71**, 034504 (2005), [arXiv:hep-lat/0405029](#); M. Cheng *et al.*, The Transition temperature in QCD, *Phys. Rev. D* **74**, 054507 (2006), [arXiv:hep-lat/0608013](#); Y. Aoki, G. Endrodi, Z. Fodor, S. D. Katz, and K. K. Szabo, The Order of the quantum chromodynamics transition predicted by the standard model of particle physics, *Nature* **443**, 675 (2006), [arXiv:hep-lat/0611014](#); Y. Aoki, Z. Fodor, S. D. Katz, and K. K. Szabo, The QCD transition temperature: Results with physical masses in the continuum limit, *Phys. Lett. B* **643**, 46 (2006), [arXiv:hep-lat/0609068](#); S. Borsanyi, Z. Fodor, C. Hoelbling, S. D. Katz, S. Krieg, C. Ratti, and K. K. Szabo (Wuppertal-Budapest), Is there

- still any T_c mystery in lattice QCD? Results with physical masses in the continuum limit III, [JHEP **09**, 073, arXiv:1005.3508 \[hep-lat\]](#).
- [9] A. M. Polyakov, Thermal Properties of Gauge Fields and Quark Liberation, [Phys. Lett. B **72**, 477 \(1978\)](#); G. 't Hooft, On the Phase Transition Towards Permanent Quark Confinement, [Nucl. Phys. B **138**, 1 \(1978\)](#); A. Casher, Chiral Symmetry Breaking in Quark Confining Theories, [Phys. Lett. B **83**, 395 \(1979\)](#); T. Banks and A. Casher, Chiral Symmetry Breaking in Confining Theories, [Nucl. Phys. B **169**, 103 \(1980\)](#); J. Braun, L. M. Haas, F. Marhauser, and J. M. Pawłowski, Phase Structure of Two-Flavor QCD at Finite Chemical Potential, [Phys. Rev. Lett. **106**, 022002 \(2011\), arXiv:0908.0008 \[hep-ph\]](#); F. Xu, T. K. Mukherjee, H. Chen, and M. Huang, Interplay between chiral and deconfinement phase transitions, [EPJ Web Conf. **13**, 02004 \(2011\), arXiv:1101.2952 \[hep-ph\]](#); F. Xu and M. Huang, The chiral and deconfinement phase transitions, [Central Eur. J. Phys. **10**, 1357 \(2012\), arXiv:1202.5942 \[hep-ph\]](#); K. Miura, T. Z. Nakano, A. Ohnishi, and N. Kawamoto, Chiral and deconfinement transitions in strong coupling lattice QCD, [PoS **LATTICE2010**, 202 \(2010\), arXiv:1012.1509 \[hep-lat\]](#).
- [10] J. B. Kogut and L. Susskind, Hamiltonian Formulation of Wilson's Lattice Gauge Theories, [Phys. Rev. D **11**, 395 \(1975\)](#); H. Kluberg-Stern, A. Morel, O. Napoly, and B. Petersson, Flavors of Lagrangian Susskind Fermions, [Nucl. Phys. B **220**, 447 \(1983\)](#); A. Morel and J. P. Rodrigues, How to Extract QCD Baryons From a Lattice Theory With Staggered Fermions, [Nucl. Phys. B **247**, 44 \(1984\)](#).
- [11] M. A. Clark and A. D. Kennedy, The RHMC algorithm for two flavors of dynamical staggered fermions, [Nucl. Phys. B Proc. Suppl. **129**, 850 \(2004\), arXiv:hep-lat/0309084](#); Accelerating Staggered Fermion Dynamics with the Rational Hybrid Monte Carlo (RHMC) Algorithm, [Phys. Rev. D **75**, 011502 \(2007\), arXiv:hep-lat/0610047](#).
- [12] G. S. Bali and K. Schilling, Static quark - anti-quark potential: Scaling behavior and finite size effects in SU(3) lattice gauge theory, [Phys. Rev. D **46**, 2636 \(1992\)](#); G. S. Bali, B. Bolder, N. Eicker, T. Lippert, B. Orth, P. Ueberholz, K. Schilling, and T. Struckmann (TXL, T(X)L), Static potentials and glueball masses from QCD simulations with Wilson sea quarks, [Phys. Rev. D **62**, 054503 \(2000\), arXiv:hep-lat/0003012](#); B. Orth, T. Lippert, and K. Schilling, Finite-size effects in lattice QCD with dynamical Wilson fermions, [Phys. Rev. D **72**, 014503 \(2005\), arXiv:hep-lat/0503016](#).

- [13] R. Sommer, A New way to set the energy scale in lattice gauge theories and its applications to the static force and α_s in SU(2) Yang-Mills theory, *Nucl. Phys. B* **411**, 839 (1994), [arXiv:hep-lat/9310022](#); M. Cheng *et al.*, The QCD equation of state with almost physical quark masses, *Phys. Rev. D* **77**, 014511 (2008), [arXiv:0710.0354 \[hep-lat\]](#); A. Bazavov *et al.* (MILC), Results for light pseudoscalar mesons, *PoS LATTICE2010*, 074 (2010), [arXiv:1012.0868 \[hep-lat\]](#).
- [14] A. Bazavov *et al.*, The chiral and deconfinement aspects of the QCD transition, *Phys. Rev. D* **85**, 054503 (2012), [arXiv:1111.1710 \[hep-lat\]](#).
- [15] C. Gattringer and C. B. Lang, *Quantum chromodynamics on the lattice*, Vol. 788 (Springer, Berlin, 2010).
- [16] U. Wolff (ALPHA), Monte Carlo errors with less errors, *Comput. Phys. Commun.* **156**, 143 (2004), [Erratum: *Comput.Phys.Commun.* 176, 383 (2007)], [arXiv:hep-lat/0306017](#).